Am J Cancer Res 2016;6(5):1053-1065
www.ajcr.us /ISSN:2156-6976/ajcr0024145

Original Article

A prostate-specific antigen-dependent fusion polypeptide inhibits growth of prostate cancer cells *in vitro* and *in vivo*

Xiang Zhang[1,2*], Yueyun Ma[1*], Hua Wei[1], Bin Li[1], Fengjing Xiao[1], Jing Yang[1], Qiaohong Yue[1], Angang Yang[2], Xiaoke Hao[1]

[1]*Department of Clinical Laboratory Medicine, Xijing Hospital, Fourth Military Medical University, Xi'an 710032, China;* [2]*Department of Immunology, Fourth Military Medical University, Xi'an 710032, China.* [*]*Equal contributors.*

Received January 15, 2016; Accepted February 22, 2016; Epub May 1, 2016; Published May 15, 2016

Abstract: Polypeptide APP8 is a prostate-specific antigen (PSA)-activated prodrug that was designed to synergize the effects of the Bcl-2 homology domain 3 (BH3) peptide, K237 and the DG2 peptide. The aim of this study is to evaluate its biodistribution and anticancer effect in vitro and in vivo. In this study, APP8 and each component peptide were synthesized. The biodistribution was identified using con-focal microscopyin both PSA^+ cell line and PSA^- cell line *in vitro*. Then cell cycle, MTT and in-cell western blot were accessed to analyze the effect mechanisms. Finally, xenografts were used to confirm the anticancer effect *in vivo*. Here, it was shown that APP8 was hydrolyzed and BH3 was released into the nucleus, while K237 and DG2 were located predominantly in the cytoplasm, only in LNCaP cells (PSA^+), but not PC3 cells (PSA^-). K237 and DG2 could induce cell apoptosis through decreasing the phosphorylation of ERK-2 and Flk-1. APP8 also caused the death of LNCaP cells, and was predominantly dependent on BH3 in vitro. In addition, It was noted that as the tumor grew in vivo, APP8 could inhibit the tumor volume to 77.3%, mainly depending on K237 and DG2 via inhibition of the growth of vascular endothelial cells.Our results suggested that APP8 could promote prostate cancer cell death and stop prostate cancer growth via synergizing apoptosis induction of tumor cell and inhibition of the growth of vascular endothelial cells. It provides a novel candidate prodrug for specific therapy of prostate cancer.

Keywords: Prostate-specificantigen, APP8, Bcl-2 homology domain 3, ERK-2, Flk-1

Introduction

Prostate cancer is the most common malignancy in men, and the second leading cause of death from cancer in western countries [1]. The incidence has increased to become the second most frequently diagnosed cancer, and the third most common cause of death from cancer in men in developing countries [2]. Traditionally, there have been several forms of treatment, such as prostatectomy, chemotherapy, radiotherapy, and hormone therapy, either by orchiectomy or anti-androgenic agents. However, these are unsatisfactory because they lack specificity, and lots of adverse effects on the healthy surrounding tissues and quality of life [3]. There is currently no effective cure for late-stage hormone (androgen)-refractory prostate cancer [4].

To enhance the anti-tumor efficacy and reduce the negative impact of prostate cancer drugs, numerous targeting therapies have been introduced, including ADEPT (antibody-directed enzyme prodrug therapy), GDEPT (gene-directed enzyme prodrug therapy) and PMT (prodrug-mono therapy). The cytotoxic agents such as chemical drugs and biological medicinal products can be released from nontoxic prodrugs at the tumor site, either by targeted antibody-enzyme conjugates, enzyme-coding genes, or tumor markers in cancerous tissues [5], likegsemino protein (SM) [6], prostate-specific membrane antigen (PSMA) [7], and prostate-specific antigen (PSA) [8].

PSA is a serine protease with chymotrypsin-like activity produced by prostate epithelial cells. Its normal function is to liquefy gelatinous semen

after ejaculation, allowing spermatozoa to navigate through the uterine cervix more easily. There is very little PSA (1,000-10,000-fold lower concentration) in the circulating blood, where it is inactivated because of binding to abundant serum protease inhibitors [9]. However, in prostate cancer it was overexpressed to degrade extracellular matrix glycoproteins fibronectin and laminin to facilitate invasion of prostate cancer cells [10]. The exclusive presence of high levels of active PSA within prostate cancer sites makes PSA an attractive target for several prodrug designs [11-13]. In these, chemical substances such asdesacetyl-vinblastine [11], thapsigargin [12], and N-(2-hydroxypropyl)methacrylamide [13] are covalently linked to a peptide that can be hydrolyzed by PSA.

Besides the chemical drugs above, biological medicinal products are also novel candidates that may stop cancer growth and promote cancer cell death by inducing apoptosis or anti-angiogenesis. Bcl-2 homology domain 3 (BH3) of BH3 only protein BID or BIM canfunction as a uniquely important cell-death inducer by initiating mitochondrial membrane permeabilization and subsequent cytochrome C efflux through activating the multi-BH domain proteins BAX and BAK [14, 15]. Some cell growth factors such as vascular endothelial growth factor (VEGF) or basic fibroblast growth factor (bFGF) are highly expressed in many tumor cells and are important targets. Antiangiogenicagents such as antibodies, inhibitor peptides, and siRNA against these factors have emerged from extensive basic and clinical research on cancer therapy [16-18]. DG2 peptide, which was screened from phage-epitope libraries, blocks binding of bFGF to its high-affinity receptor ERK-2, and inhibits basal and bFGF-induced proliferation of vascular endothelial cells [19]. K237 interferes with the VEGF-Flk-1 interaction by binding to Flk-1 (a kinase domain receptor) with high affinity and specificity, and inhibits proliferation of cultured primary human umbilical vein endothelial cells [20].

A similar polypeptide, BSD352, which combines BH3-TAT, DG2 and SP5.2, has a good inhibitory effect on prostate cancer through apoptosis induction [8]. However, the synergistic effect and mechanism of action have not been demonstrated. Here, we synthesized a novel fusion polypeptide including BH3, DG2 and K237, which were linked to each otherusing PSA-cleaved peptide. The localization and anti-prostate cancer effect of each peptide were identified to be PSA dependent. Furthermore, APP8 was proved to inhibit growth of prostate cancer *in vitro* and *in vivo* by different mechanisms.

Materials and methods

Cell lines and cell culture

The human androgen-independent prostate cancer cell lines PC-3 (No.3115CNCB00313, Generation 23), and androgen-dependent prostate cancer cell lines LNCaP (No.3111C00-01CCC000040, Generation 50) were purchased from Beijing North Carolina Chuanglian Biological Technology Research Institute of China. All the cell lines were cultured as monolayers in RPMI1640 medium supplemented with 10% heat-inactivated fetal calf serum (FCS; both from Life Technologies, Grand Island, NY, USA), 100 μg/mL penicillin and 100 μg/mL streptomycin at 37°C in a humidified 5% CO_2 incubator. Characterization of the cell lines was performed by testing the expression of PSA using electrochemical luminescence method on a RocheCobas E601 module immunology analyzer (Roche Group, Basel, Switzerland).

Peptide design and preparation

The basic peptide BH3-HIV-TAT, VEGF antagonist K237, bFGF antagonist DG2, and the polypeptide APP8, APPKB and APPBD were synthesized by the solid phase peptide synthesis method at GL Biochem (Shanghai. China) Ltd. Before that an 8 KD peptide was identified after its coding sequence was cloned and expression in E. coli BL21. The purified peptides APPKB and APPBD were labeled with fluorescein isothiocyanate (FITC) at the N terminus and rhodamineB at the C terminus (**Figure 1A**). Protein Folding Rates of any peptides were predicated using SFOLDRATE web service at http://gila.bioengr.uic.edu/lab/.

Immunofluorescence staining

LNCaP and PC3 cells were cultured on coverslips in RPMI1640 medium supplemented with 10% FCS, and fixed with a freshly prepared paraformaldehyde (PFA) solution [4% in phos-

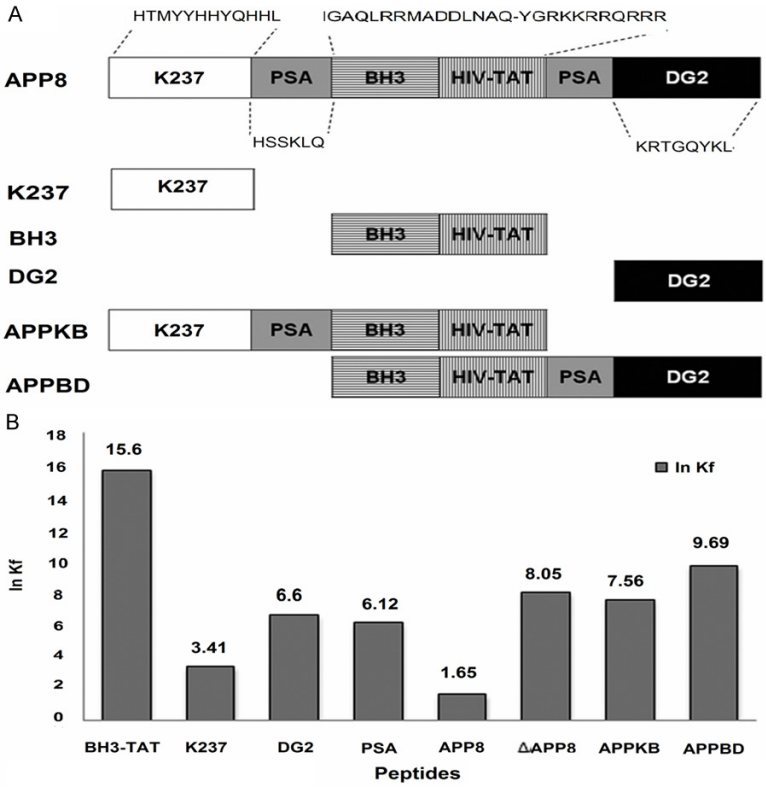

Figure 1. Schematic diagram of synthesized APP8 polypeptide and its component peptides. A. APP8 was designed synergizing BH3, DG2 and K237, which were linked to each other using PSA-cleaved peptide. APPKB and APPBD labled with FITC and rhodamineB were also synthesized to observe localization of the peptides. B. The lnKfs of BH3-TAT, K237, and DG2.

phate-buffered saline (PBS), pH 7.4] for 30 minutes at room temperature, and permeated with 0.1% Triton X-100 (Sigma, St. Louis, MO, USA) for 15 minutes on ice. The localization of each peptide (BH3-HIV-TAT, K237 and DG2) was checked first. Then, 100 μM APPKB or APPBD was added to the cells. 4',6-Diamidino-2-phenylindole (DAPI; Molecular Probes, Eugene, OR, USA) was used for nuclear staining. The distribution of FITC and rhodamineB fluorescence in live cells was observed by MRC-1024 laser scanning confocal microscopy imaging (LSCM; Bio-Rad Laboratories, Hercules, CA, USA), and images of interest were saved.

In cell western blotting

Quantitative analysis of cellular extracellular signal-regulated kinase (ERK)-2, Flk-1 protein and their phosphorylation levels were carried out using a rapid and high-through put in-cell western blotting method, as previously described [21]. Briefly, 1,000 LNCaP cells/well were seeded in a clear-bottomed 96-well plate and grown for 24 hours at 37°C/5% CO_2. The cells were fixed in 4% PFA. After permeabilization with 0.1% Triton X-100 in PBS (200 mL/well), the wells were incubated with goat anti-ERK-2, anti-p-ERK, anti-Flk-1, anti-p-Flk-1 and anti-β-actin antibody (1:500, Santa Cruz Biotechnology, Santa Cruz, CA, USA) and subsequently washed with 0.1% Tween-20 in PBS. Donkey anti-goat DyLight 488 secondary antibody (1:1,000) was added. After washing, the plates were imaged on an Odyssey infrared scanner (LI-COR Biosciences, Lincoln, NE, USA) in the 488 nm wavelength channels. The score of p-ERK and p-Flk-1 was normalized by OD_{488} of β-actin.

Chromatin staining with Hoechst 33258

Apoptosis was observed by chromatin staining with Hoechst 33258 as previously described [22]. After 72 hours of treatment with 800 μM of APP8 recombinant protein, LNCaP and PC3 cells were washed with ice-cold PBS, fixed with 4% PFA in PBS for 10 minutes at room temperature. Afterwards the cells were stained for 10 minutes with Hoechst 33258 (5 mg/L; Sigma, At Louis, MO, USA), they were washed and observed with an Olympus BX-60 fluorescence microscope (Olympus Medical Systems, Tokyo, Japan) by an observer blind to the cell treatment.

MTT assay for cell proliferation

PC-3 and LNCaP cells were grown to confluence in full RPMI1640 medium and harvested by trypsinization at 37°C for 5 minutes. A suspension of 1×10^4 cells in RPMI1640 medium was added to each well of 96-well plates and incubated for 24 hours at 37°C in an atmosphere of 5% CO_2. The cells were treated with 0, 100, 200, 400, or 800 μM APP8 protein. After 48

hours of incubation, 20 μL (3-[4,5-dimethylthiazol-2-yl] -2,5-diphenyl tetrazolium bromide (MTT; 5 mg/mL in PBS; Sigma) was added to each well. The cells were incubated for a further 4 hours, followed by the addition of 150 μL dimethyl sulfoxide. Absorbance at 570 nm (A_{570}), which correlates with the number of viable cells, was measured with a Bio-Rad Model 680 microplate reader (Bio-rad, Hercules, CA, USA). The mean and standard deviations of three parallel samples were calculated and cell viability rate was calculated as Absorbance of treated cells/Absorbance of untreated control cell × 100%. All experiments were performed as three independent experiments. The same procedure was also applied to the component peptides, in which the LNCaP cells were treated with 10, 100 and 1000 mM of K237, DG2 and BH3-TAT respectively.

Xenograft mice

Male BALB/c nude mice (6-8 weeks old; 18-22 g), were purchased from the National Rodent Laboratory Animal Resources, Shanghai Branch. The tumors were established by subcutaneous injection of 3×10^6 LNCaP or PC3 cells suspended in 0.1 mL PBS into the right flanks of 10 mice. When xenografts grew to a diameter of ~5.0 mm, mice were randomly assigned to twogroups and challenged intravenously with PBS and 500 μg/kg in 0.2 ml (one treatment every 3 days for 30 days) according to the preliminary experiment at 100, 250 and 500 μg/kg concentration every one, two or three day for 30 days. Serum PSA was detected using electrochemical luminescence method on a RocheCobas E601 module immunology analyzer (Roche Group, Basel, Switzerland). The body weight of the nude mouse was recorded. The volume of the tumor was calculated with the formula (14): Tumor volume (mm^3) = $width^2$ × length/2 by measuring 2 diameters perpendicular to each other with a caliper every 5 days. Mice were sacrificed by cervical dislocation on day 30 after APP8 administration. The tumors were removed for weightingand histological staining.

Ethics statement

The animal experiment was approved by Ethical Committee of the Fourth Military Medical University (Approved No. 20130020). Animals received a standard diet and water and were cared for in accordance with the Principles of Laboratory Animal Care (NIH publication No.86-23, revised 1985) as well as the China Committee of Animal Experimentation.

Histological examination

Resected tumors were fixed in 10% neutral-buffered formalin and processed through a series of increasing ethanol concentrations for paraffin embedding. Serial sections (5 μm) were cut on a Leica RM2235 microtome (Leica Microsystems, Wetzlar, Germany). The sections were dewaxed, hydrated, and stained with hematoxylin-eosin (H&E; Dako, Carpenteria, CA, USA) and examined with a CX31 light microscope (Olympus Medical Systems).

Blood microvessel density (MVD)

Blood vessel immune staining was carried out with monoclonal CD34 antibodies (Santa Cruz Biotechnology) using the avidin-biotin-peroxidase complex (ABC) technique as described previously [23]. Immuno stained tumor sections were scanned at low magnification (40×) and the 3 most densely vascular areas ("hot spots") were photographed at 200× magnification. IntratumoralMVD was assessed by counting the total number of microvessels found in that area (0.720 mm^2), as described previously [24].

Statistical analysis

Statistical analyses were performed with the SPSS for Windows version 11.5 (SPSS, Chicago, IL, USA). The comparisons between every treatment groups and control were made by the Wilcoxon matched-pairs signed-ranks test first. Finally the cell viability rates, tumor volume, tumor weight, and MVD were analyzed using the Kaplan-Meier method. $P < 0.05$ was considered statistically significant.

Results

Folding rates of the peptides

Each peptide (**Figure 1A**) was obtained at >98% purity. To clarify thenative topologies of these peptides, we used a method described by Ouyang and Liang [25] to calculate the folding rates of the peptides based on the geometric contact and amino acid sequence. As shown in **Figure 1B**, the lnKfs of BH3-TAT, K237, and DG2 were 15.6, 3.41, and 6.6, respectively. When

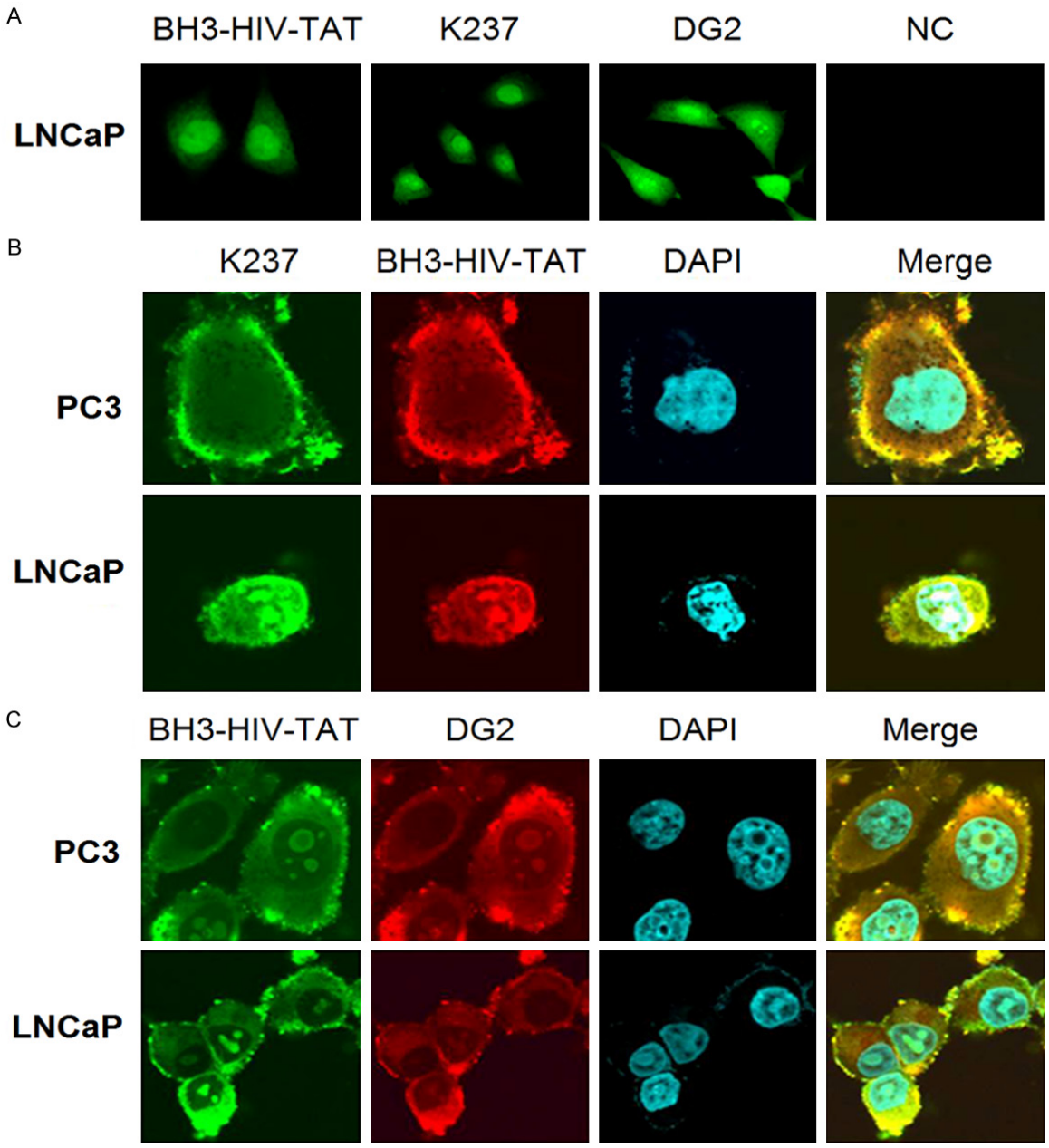

Figure 2. Localization of the functional peptides on prostate cancer cells. A. Distribution of BH3-HIV-TAT, K237 and DG2 in LNCaP cells. B. Distribution of K237 and BH3-TAT peptides from APPKB in LNCaP cells. Cells were exposed to APPKB labeled with FITC and rhodamineB on each side, counterstained with DAPI, and observed by LSCM (magnification: 200×). C. Distribution of BH3-TAT and DG2 peptides from APPBD in LNCaP cells. The cells were exposed to APPBD labeled with FITC and rhodamineB on each side, counterstained with DAPI, and observed by LSCM (magnification: 200×).

the folding rate of APP8 was 1.65, the lnKf increased to 8.05, if the three peptides were linked into DAPP8 without PSA-cleaved peptide. That is almost the average of the three individual peptides. Similarly, APPKB and APPBD had lnKfs of 7.56 and 9.69 respectively. This indicates that APP8 is less active before its peptides are cleaved.

Distribution of functional peptides in prostate cancer cells

It was confirmed that about 8.8-97.07 and 72.16-216.4 ng/ml PSA could be detected in the supernatant and cytoplasma of LNCaP respectively, but none could be detected in the supernatant of PC3 (Supplementary Table 1).

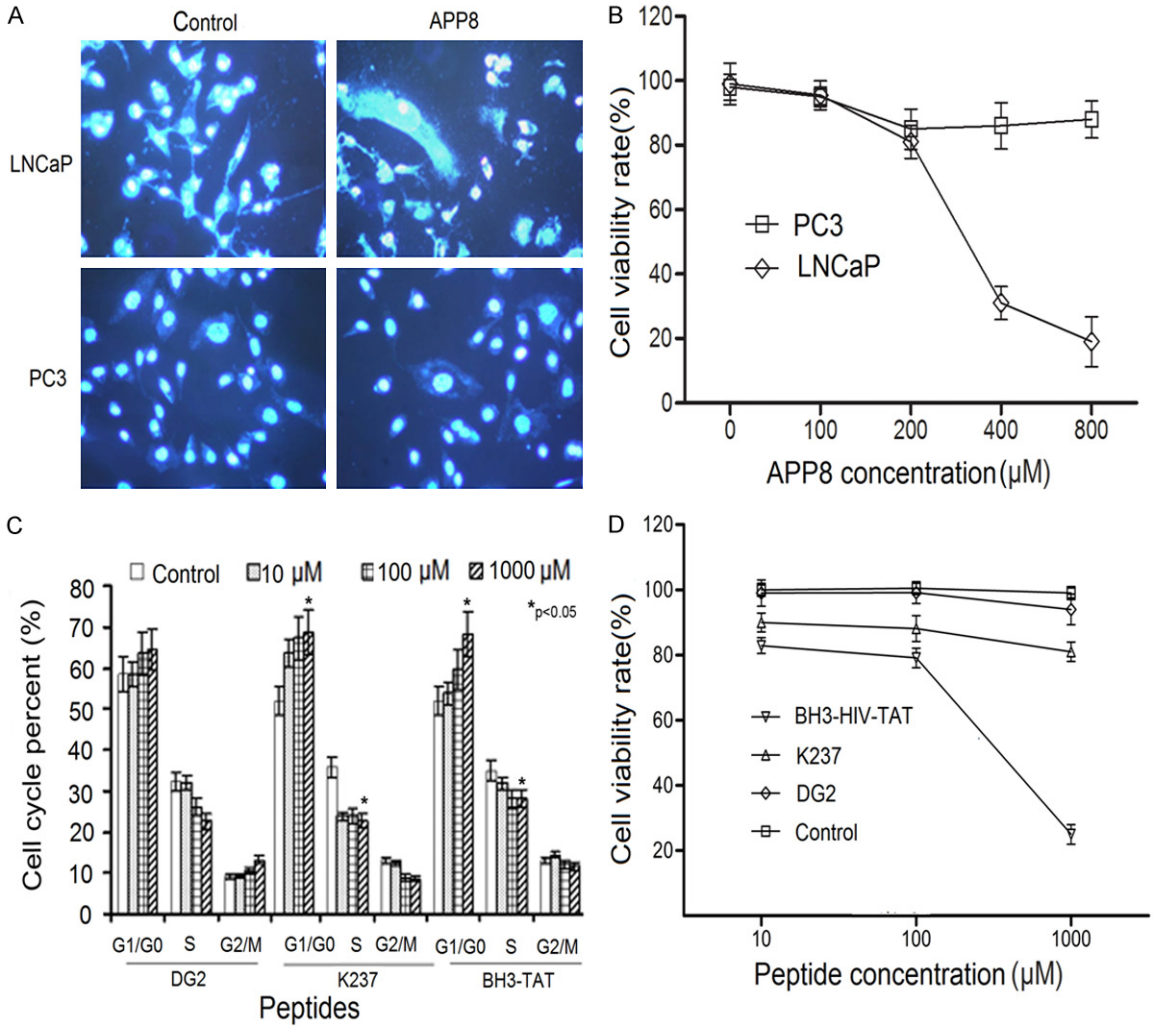

Figure 3. The effect of peptides on apoptosis of prostate cancer cells. Apoptosis of PC3 and LNCaP cells induced by APP8 was detected after the cells were exposed to APP8 for 48 hours, using chromatin staining with Hoechst 33258 (magnification: 200×) (A). The cell viability was measured using the MTT method (B). The cell cycle was analyzed by measuring cellular DNA content on a flow cytometer after LNCaP cells were exposed to K237, DG2 and BH3-TAT (C). MTT assay was carried out to evaluate cell viability (D).

Then the distribution of K237, BH3-HIV-TAT and DG2 was observed in LNCaP and PC3 cells to identify the cleavage of PSA. As shown by **Figure 2A**, BH3-HIV-TAT was located mainly in nucleus, K237 located in both cytoplasm and nucleus, and DG2 located mainly in the cytoplasm of LNCaP. In **Figure 2B** and **2C**, FITC (green) and rhodamineB (red) refer to K237 and BH3-HIV-TAT in APPKB, while they indicated BH3-HIV-TAT and DG2 in APPBD. Both K237 and BH3-HIV-TAT were equally located in the cytoplasm of PC3 cells, but not the nucleus. Both BH3-HIV-TAT and K237 were detected in the nucleus and cytoplasm of LNCaP cells, same as the peptide alone(**Figure 2B**). BH3-HIV-TAT and DG2 were located in the cytoplasm of PC3 cells. However in LNCaP cells, BH3-HIV-TAT was internalized into the nucleus, while DG2 was mainly maintained in the cytoplasm (**Figure 2C**). Over laying the red or green fluorescence and DAPI staining of the nucleus confirmed the nuclear distribution of BH3-HIV-TAT. It was confirmed that APPBD and APPKB could only be cleaved in LNCaP, which secreted PSA.

The activity of APP8 and the functional peptides in vitro

To further check the action of APP8, MTT was carried out in both PC3 and LNCaP. Hoechst 33258 staining revealed the typical features of

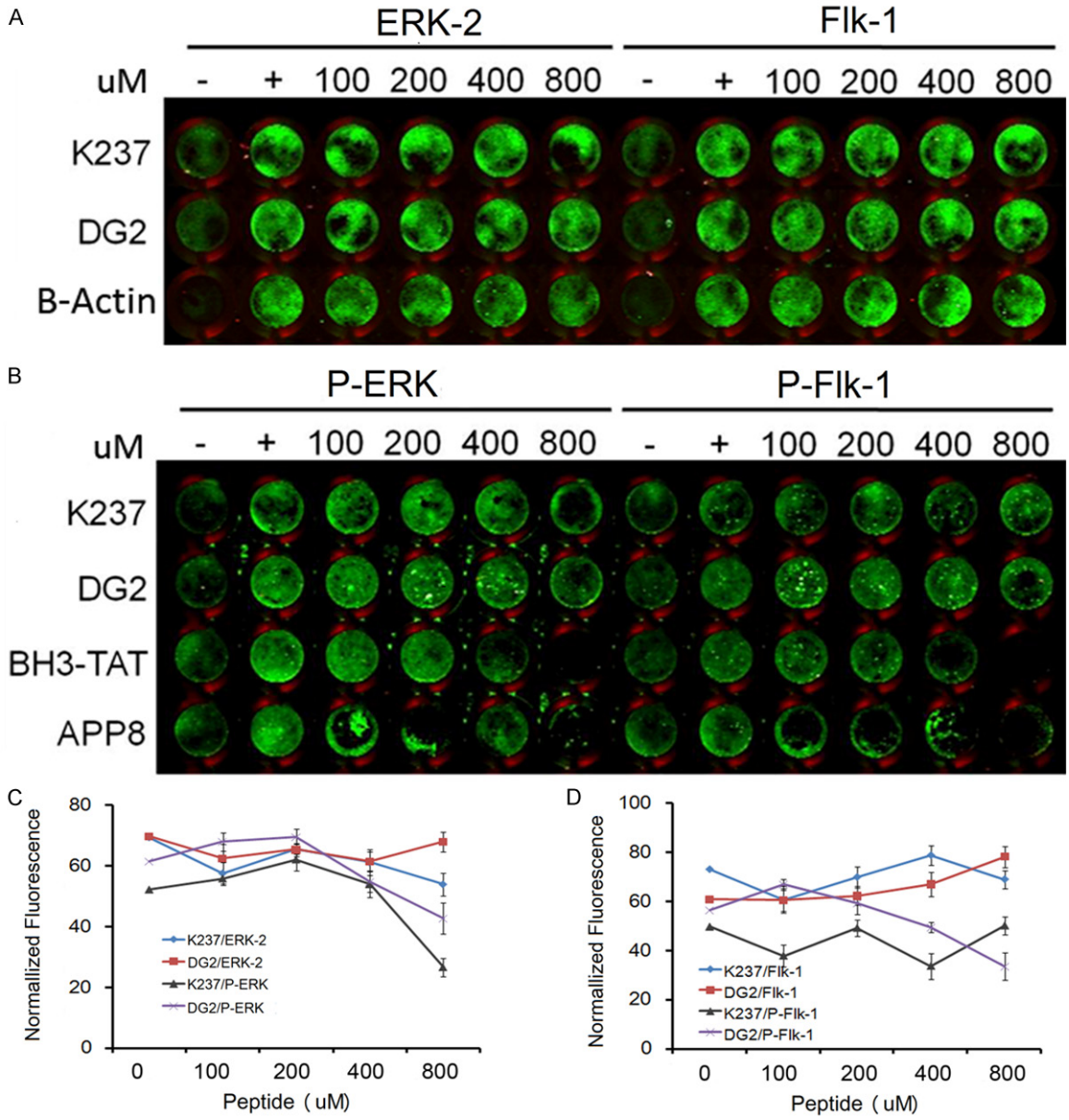

Figure 4. In-cell western blotting of ERK2, Flk-1, p-ERK and p-Flk-1 in LNCaP cells exposed to peptides. LNCaP cells were exposed to, BH3-TATand APP8. ERK-2 and Flk-1 were measured after the cells were exposed to DG2 and K237 for 48 hours (A). p-ERK and p-Flk-1were measured after the cells were exposed to DG2, K237, BH3-TAT and APP8 for 48 hours (B). There was only a second antibody in the "–" lane. There were both first and second antibodies but no peptides in the "+" lane. Each peptide was added at a concentration of 100, 200, 400, and 800 mM. The fluorescence of each well was normalized with that of anti-β-actin in the same lane. Each experiment was carried out 3 times along with statistical analysis (C, D).

apoptosis, including cell shrinkage, chromatin condensation, and hypodiploid genomic DNA content in PSA-secreting LNCaP cells exposed to 800 μM APP8 for 48 hours after its stability was confirmed in LNCaP cells (Supplementary Figure 1). However, the same features were absent in non-PSA-secreting PC3 cells exposed to APP8 (**Figure 3A**). MTT assay showed that the viability of the PSA-secreting cell line LNCaP significantly decreased to 22% at 48 hours after treatment with 800 μM APP8 (**Figure 3B**). However, viability of the non-PSA-secreting cell lines PC3 treated with the same dose of APP8 barely changed from 95% to 87% (**Figure 3B**). It was suggested that the activity of APP8 was PSA dependent.

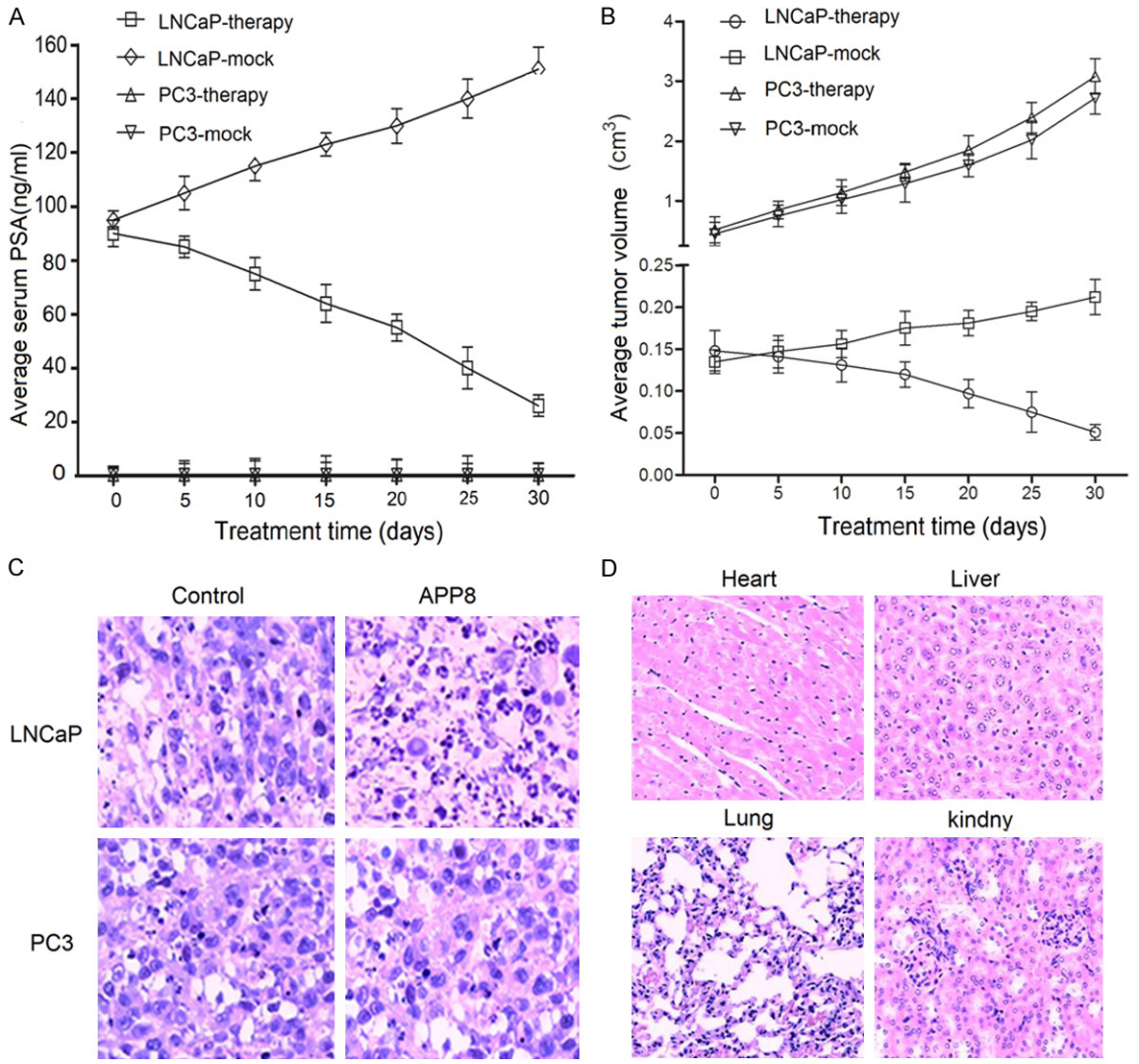

Figure 5. Effect of APP8 on proliferation of prostate cancer cells in vivo. Each 10 mice were subcutaneously injected with 3 × 10^6 LNCaP or PC3 cells, followed by intravenous 100 μg APP8 every 3 days for 30 days. Serum PSA level was evaluated (A). Tumor volume (B) was measured at nescropsy of thexenografts. Sections of tumor xenografts and other tissues (heart, liver, lung, and kidney) were examined histologically at 200× magnification (C, D).

To demonstrate the inhibitory effects of K237 and DG2 on prostate cancer cell proliferation, the cell cycle was analyzed using flow cytometry. K237 and BH3-TAT but not DG2 arrested cell cycle progression of LNCaP cells at the G1/G0 and S phases ($P < 0.05$) (**Figure 3C**). Similarly, MTT assay showed that the BH3-TAT peptide (10, 100 or 1,000 μM) reduced the viability of LNCaP cells to 82.9%, 79.1% and 25.0%, respectively, at 24 hours (**Figure 3D**). The K237 peptides reduced it to 91.2%, 85.1% and 77.6%. Both BH3-TAT and K237 inhibited proliferation of LNCaP cells in a concentration-dependent manner. In contrast, DG2 did not show any significant effect.

FGF and VEGF pathwayinhibited by peptides

To confirm whether the FGF and VEGF pathways were blocked, p-ERK-2 and p-Flk-1, which are active receptors of bFGF and VEGF respectively, were detected using in-cell western blotting. The results in **Figure 4A**, **4C** showed that K237 and DG2 did not affect expression of ERK-2 and Flk-1. However, when 800 mM K237 was added, the quantity of p-ERK decreased by 2-folds (normalized fluorescence intensity 72 to 36) significantly. Also, the normalized fluorescence intensity of p-Flk-1 decreased from 81 to 52 by 800 mM DG2 (**Figure 4B**, **4D**). At the same time, BH3-TAT caused the death of LNCaP

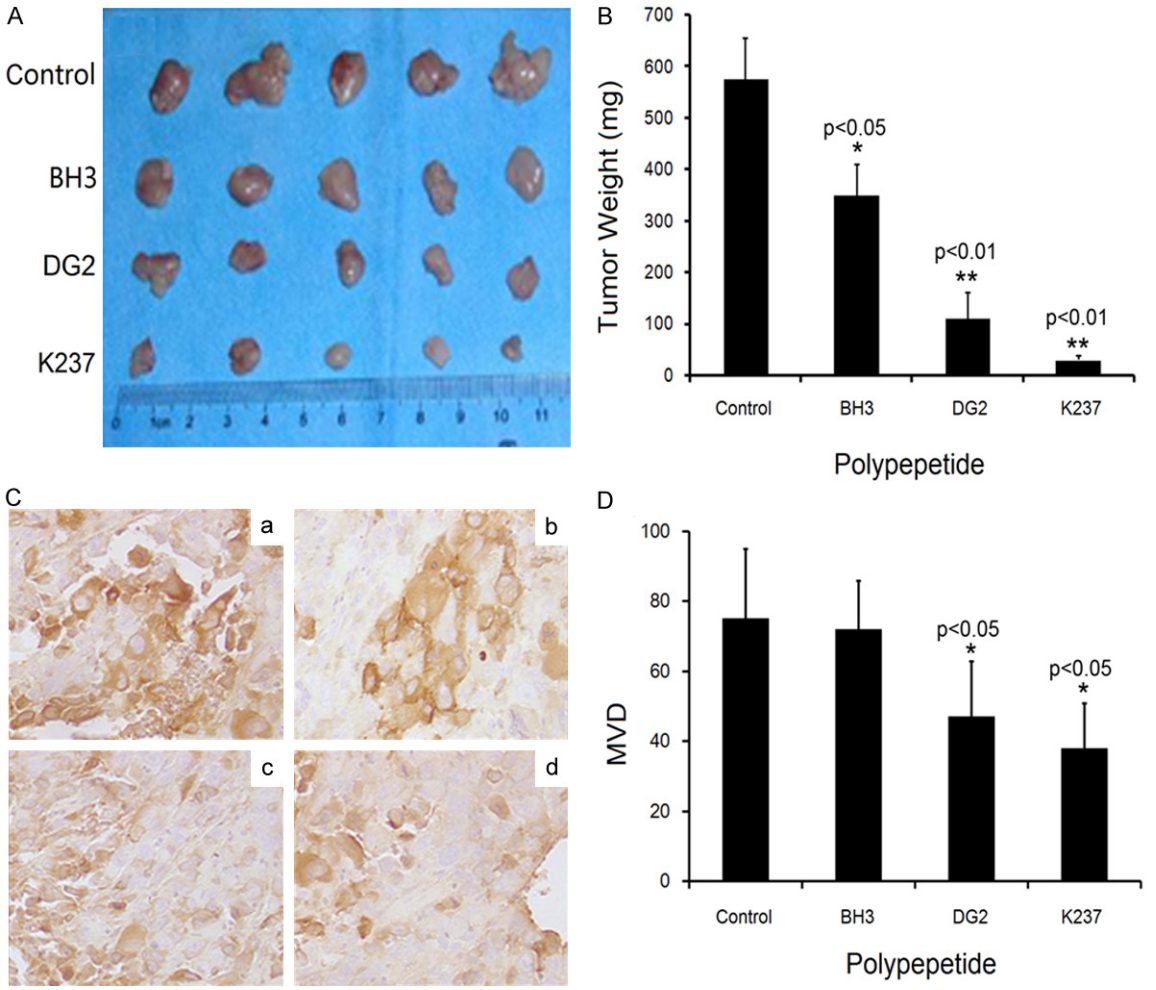

Figure 6. Effect of peptides on proliferation of prostate cancer cells in vivo. Each 7 mice were subcutaneously injected with 3 × 10^6 LNCaP cells. Mice were intravenously administered with PBS, 1000 μM BH3, DG2 and K237 every 3 days for 30 days. Tumor xenografts were separated and the tumor weights were checked (A, B). Blood vessel immunostaining was carried out with monoclonal CD34 antibodies using the ABC technique. Immunostained tumor sections were scanned at low magnification (40×) and the 3 most densely vascular areas (hot spots) were photographed at 200× magnification (C, D).

cells in a dose-dependent manner, with 800 mM resulting in the death of all cells. Although a concentration of only 100 or 200 mM APP8 achieved the same effect. Comparing with the low level of cell death induced by K237 and DG2, APP8 caused more cell death than BH3-TAT alone. This suggests that apoptosis is the main cause of cell death *in vitro*, although it may also be induced by a synergistic effect of K237 and DG2.

Cytotoxicity of APP8 in prostate cancer xenografts

In addition to *in vitro* testing, 10 nude mice bearing the LNCaP or PC3 xenograft were treated with APP8 for 30 days *in vivo*. Before that its stability was confirmed in mice up to 72 hrs (Supplementary Figure 2). The results showed that in **Figure 3C**, serum PSA level in LNCaP xenograft significantly decreased from 90 ng/ml to 30 ng/ml after APP8 treatment, while the PSA increased from 90 ng/ml to 150 ng/ml in mock group. At the same time, the average volume of the tumor decreased by 77.3% in APP8 treatment group in comparison with the mock group (**Figure 5A**, **5B**). However, the changes in PSA level, and tumor volume in nude mice bearing the non-PSA-secreting PC3 xenograft were not significantly different between the APP8- and mock-treated groups. Gross observation revealed significant tumor necrosis in the

LNCaP xenografts treated with APP8. The tumor tissue was less solid and became friable, and only the outer membrane of the tumor and small amounts of the tumor were left in the periphery of the tumor xenografts. H&E staining revealed necrotic tissue in PSA-secreting LNCaP xenografts treated with APP8 (**Figure 5C**), while there was vigorous tumor cell growth in non-PSA-secreting PC3 cells. However, no obvious cytotoxicity was observed in the vital organs such as the heart, liver, lung and kidney of the xenograft mice(**Figure 5D**). This result supported the low folding rates of APP8, which means less activity before being cleaved by PSA.

Proliferation of prostate cancer cells inhibited by peptides in vivo

To further understand the role of component peptides of APP8 *in vivo*, 0.2 ml of 1 mM DG2, K237 or BH3-TAT was also applied to 6 or 7 xenograft mice. Surprisingly, the tumor weights significantly decreased by DG2 and K237 in addition to BH3-TAT. This differed greatly from their cellular effects *in vitro*. DG2 reduced tumor weight by 81.2%, and K237 by 90.1% as compared to the mock-treated group, which was much stronger than the 36.4% reduction with BH3-TAT (**Figure 6A**, **6B**). In contrast to the *in vitro* tests, inhibition of proliferation by K237 and DG2 contributed more to tumor growth arrest than apoptosis induced by BH3 did.

Because of the roles of FGF and VEGF pathway in angiogenesis, MVD in each tumor was compared. BH3-TAT did not change MVD. However, DG2 reduced MVD by 34.7%, and K237 reduced MVD by 49.3% compared with the mock-treated group (**Figure 6C**, **6D**). It suggested that the tumor growth arrest role of K237 and DG2 in vivo was performed through antiangiogenesis of the tumor.

Discussion

As a prodrug, APP8 should be non-cytotoxic before being localized in PSA-secreting prostate cancer cells. For this goal, the folding rates of the peptides were evaluated to predict their topologies. Protein folding is the process of transformation of one-dimensional linear information encoded in the amino acid sequence into a functional 3D structure [26]. The folding rate is correlated well with the long range order, effective contact order, absolute contact order, total contact distance, a chain topology parameter, and the effective length of the protein [25]. Analysis of APP8 showed a distinguishable lower lnKf from the high lnKf of the individual peptides (**Figure 1**). This indicated that APP8 did not fold as well as its components did. Therefore, the activity of the original peptides would be lost completely or incompletely in APP8. This was confirmed by the cellular and xenograft experiments, in which APP8 did not show induction of apoptosis of PC3 cells (**Figure 4C**), did not inhibit PC3 xenograft tumor growth (**Figure 4F**), and did not show cytotoxicity to the heart, liver, spleen, lung or kidney of the xenograft mice.

PSA-specific small peptides have been designed and conjugated to doxorubicin or vinblastine to generate inactive prodrugs that can be selectively activated by PSA-producing tumors both *in vitro* and *in vivo* [27, 28]. Recently, an albumin-doxorubicin prodrug, in which albumin acted as the drug carrier, was introduced to improve cancer chemotherapy [29]. In this study, APP8 was hydrolyzed by PSA *in vitro* and *in vivo*. Both APPKB and APPBD released BH3-TAT into the nucleus of PSA-secreting LNCaP cells, but not in PC3 cells that did not secrete PSA. APP8 induced apoptosis of LNCaP but not PC3 cells. Furthermore, APP8 inhibited the growth of LNCaP but not PC3 xenografts. It was demonstrated that APP8 was a tissue specific prodrug that could be activated only by PSA to suppress the growth of prostate cancer. Here, the TAT protein transduction domain (PTD) used to fuse with BH3 was derived from amino acids 47-57 of the HIV TAT protein for their ability to cross the cell membrane and deliver macromolecular cargo in cell culture and *in vivo* [30]. It avoids many drawbacks of traditional viral delivery systems in gene therapy, such as low delivery efficiency, serious toxicity, and immunogenicity. Recent studies showed that the TAT-survivin peptide, which results in apoptotic cell death specifically in tumor cells, could be used in the treatment of several cancers, including prostate, breast, leukemia, melanoma and glioma [31].

Improving the targeted therapy of PSA-activated prodrugs trategies may rely on some cytotoxic effectors to exert an anticancer function efficiently [29]. The molecules used in this experi-

ment were proapoptotic BH3 domain with an HIV-TAT transduction domain, and VEGF and bFGF inhibitors K237 and DG2. It was hopefully designed to suppress the tumor from both inside and outside the cell.

In vitro, APP8 induced a high level of LNCaP cell death, mainly dependent on BH3. This was because BH3 could induce apoptosis [8], cell cycle arrest at the G1/G0 stage, and further suppress cell growth in a concentration-dependent manner.

VEGF and bFGF, two important proangiogenic factors, are involved in tumor angiogenesis and tumor cell proliferation [32]. Inhibition of the interaction between VEGF, bFGF and their corresponding receptors is one strategy for cancer therapy [33, 34]. K237 is an antagonist of the VEGF receptor KDR/Flk-1, and DG2 is an inhibitor of bFGF through blocking binding to the high-affinity receptor ERK1/2. They inhibit the phosphorylation of the receptors in LNCaP cells. Thus, it was expected that APP8, the fusion of BH3-TAT, K237 and DG2, would induce more cell death than BH3-TAT alone. In addition, it was confirmed that K237 inhibited proliferation of LNCaP cells in a concentration-dependent manner. This result was in agreement with the study of Deezagi *et al*, [35] which showed that hVEGF-siRNA significantly induced ~34% more apoptosis of DU-145 cells than the controls at 72 hours [35]. This suggests that anti-hVEGF suppresses the growth of endothelial cells as well as prostate cancer cells.

It was surprising that APP8 showed different mechanisms *in vitro* and *in vivo*. Xenograft tests showed that BH3 peptide had a suppression rate of only 36.4%, which was less than that of DG2 and K237 (81.2% and 90.1%, respectively). This was similar to the studies in which DG2 alone inhibited aortic endothelial cell growth by 70% [35], and K237 only reduced breast tumor weight by 70% *in vivo* [36]. The *in vivo* effect was exerted through inhibition of microvessel growth by DG2 and K237. They reduced MVD by 34.7% and 49.3% respectively. However, BH3 had no significant rolesin changing MVD. It is suggested that FGF and VEGF pathway-dependent microvessels are important for tumor tissue growth *in vivo*. APP8 was mainly dependent on K237 and DG2 peptides to inhibit the growth of prostate cancer *in vivo*.

Our results demonstrated that the PSA-activated, TAT-delivered polypeptide selectively delivered the therapeutic peptide into specific tumor cells. Because prostate cancer can be found at both early and later stage, inducing apoptosis or anti-angiogenesis does not eventually eliminate the tumor cells. Combining inhibition of tumor angiogenesis and simultaneously inducing tumor apoptosis may be a successful approach to treat both early and later stage human prostate carcinoma.

Acknowledgements

Grant support: National High Technology Research and Development Program of China. grants 2006AA02A24 National Natural Science Foundation of China 81372747.

Disclosure of conflict of interest

None.

Address correspondence to: Dr. Xiaoke Hao, Department of Clinical Laboratory Medicine, Xijing Hospital, Fourth Military Medical University, Xi'an 710032, China. Tel: +86-29-84775455; Fax: +86-29-82550450; E-mail: haoxkg@fmmu.edu.cn; Dr. Angang Yang, Department of Immunology, Basic Medical College, Fourth Military Medical University, Xi'an 710032, China. Tel: +86-29-84774528; E-mail: agyang@fmmu.edu

References

[1] Guo J, Evans JC and O'Driscoll CM. Delivering RNAi therapeutics with non-viral technology: a promising strategy for prostate cancer? Trends Mol Med 2013; 19: 250-61.
[2] Damber JE and Aus G. Prostate cancer. Lancet 2008; 371: 1710-1721.
[3] Nilsson S, Norlen BJ and Widmark A. A systematic overview of radiation therapy effects in prostate cancer. Acta Oncol 2004; 43: 316-381.
[4] Russell PJ and Khatri A. Novel gene-directed enzyme prodrug therapies against prostate cancer. Expert Opin Investig Drugs 2006; 15: 947-961.
[5] Tietze LF and Schmuck K. Prodrugs for targeted tumor therapies: recent developments in ADEPT, GDEPT and PMT. Curr Pharm Des 2011; 17: 3527-3547.
[6] Hao XK, Liu JY, Yue QH, Wu GJ, Bai YJ and Yin Y. In vitro and in vivo prodrug therapy of prostate cancer using anti-gamma-Sm-scFv/hCPA fusion protein. Prostate 2006; 66: 858-866.
[7] Zeng H, Wei Q, Huang R, Chen N, Dong Q, Yang Y and Zhou Q. Recombinant adenovirus medi-

ated prostate-specific enzyme pro-drug gene therapy regulated by prostate-specific membrane antigen (PSMA) enhancer/promoter. J Androl 2007; 28: 827-835.

[8] Li B, Zhang LJ, Zhang ZL, Long M, Ren JH, Lin F, Wang X, Wei JX, Dong K and Zhang HZ. Synergistic tumor growth-inhibitory effect of the prostate-specific antigen-activated fusion peptide BSD352 for prostate cancer therapy. Anticancer Drugs 2011; 22: 213-222.

[9] LeBeau AM, Singh P, Isaacs JT and Denmeade SR. Potent and selective peptidyl boronic acid inhibitors of the serine protease prostate-specific antigen. Chem Biol 2008; 15: 665-674.

[10] Webber MM, Waghray A and Bello D. Prostate-specific antigen, a serine protease, facilitates human prostate cancer cell invasion. Clin Cancer Res 1995; 1: 1089-1094.

[11] DeFeo-Jones D, Brady SF, Feng DM, Wong BK, Bolyar T, Haskell K, Kiefer DM, Leander K, McAvoy E, Lumma P, Pawluczyk JM, Wai J, Motzel SL, Keenan K, Van Zwieten M, Lin JH, Garsky VM, Freidinger R, Oliff A and Jones RE. A prostate-specific antigen (PSA)-activated vinblastine prodrug selectively kills PSA-secreting cells in vivo. Mol Cancer Ther 2002; 1: 451-459.

[12] Denmeade SR, Jakobsen CM, Janssen S, Khan SR, Garrett ES, Lilja H, Christensen SB and Isaacs JT. Prostate-specific antigen-activated thapsigargin prodrug as targeted therapy for prostate cancer. J Natl Cancer Inst 2003; 95: 990-1000.

[13] Chandran SS, Nan A, Rosen DM, Ghandehari H and Denmeade SR. A prostate-specific antigen activated N-(2-hydroxypropyl) methacrylamide copolymer prodrug as dual-targeted therapy for prostate cancer. Mol Cancer Ther 2007; 6: 2928-2937.

[14] Letai A, Bassik MC, Walensky LD, Sorcinelli MD, Weiler S and Korsmeyer SJ. Distinct BH3 domains either sensitize or activate mitochondrial apoptosis, serving as prototype cancer therapeutics. Cancer Cell 2002; 2: 183-192.

[15] Willis SN, Fletcher JI, Kaufmann T, van Delft MF, Chen L, Czabotar PE, Ierino H, Lee EF, Fairlie WD, Bouillet P, Strasser A, Kluck RM, Adams JM and Huang DC. Apoptosis initiated when BH3 ligands engage multiple Bcl-2 homologs, not Bax or Bak. Science 2007; 315: 856-859.

[16] Kerbel RS. Tumor angiogenesis. N Engl J Med 2008; 358: 2039-2049.

[17] Xie Q, Tang N, Wan R, Qi Y, Lin X and Lin J. Recombinant Snake Venom Cystatin Inhibits Tumor Angiogenesis in vitro and in vivo Associated with Downregulation of VEGF-A165, Flt-1 and bFGF. Anticancer Agents Med Chem 2013; 13: 663-71.

[18] Zhang B, Feng X, Wang J, Xu X, Lin N and Liu H. Combined antitumor effect of Ad-bFGF-siRNA and Ad-Vpr on the growth of xenograft glioma in nude mouse model. Pathol Oncol Res 2011; 17: 237-242.

[19] Yayon A, Aviezer D, Safran M, Gross JL, Heldman Y, Cabilly S, Givol D and Katchalski-Katzir E. Isolation of peptides that inhibit binding of basic fibroblast growth factor to its receptor from a random phage-epitope library. Proc Natl Acad Sci U S A 1993; 90: 10643-10647.

[20] Hetian L, Ping A, Shumei S, Xiaoying L, Luowen H, Jian W, Lin M, Meisheng L, Junshan Y and Chengchao S. A novel peptide isolated from a phage display library inhibits tumor growth and metastasis by blocking the binding of vascular endothelial growth factor to its kinase domain receptor. J Biol Chem 2002; 277: 43137-43142.

[21] Hannoush RN. Kinetics of Wnt-driven beta-catenin stabilization revealed by quantitative and temporal imaging. PLoS One 2008; 3: e3498.

[22] Yao J, Jiang Z, Duan W, Huang J, Zhang L, Hu L, He L, Li F, Xiao Y, Shu B and Liu C. Involvement of mitochondrial pathway in triptolide-induced cytotoxicity in human normal liver L-02 cells. Biol Pharm Bull 2008; 31: 592-597.

[23] Vartanian RK and Weidner N. Correlation of intratumoral endothelial cell proliferation with microvessel density (tumor angiogenesis) and tumor cell proliferation in breast carcinoma. Am J Pathol 1994; 144: 1188-1194.

[24] Delgado-Rosas F, Gaytan M, Morales C, Gomez R and Gaytan F. Superficial ovarian cortex vascularization is inversely related to the follicle reserve in normal cycling ovaries and is increased in polycystic ovary syndrome. Hum Reprod 2009; 24: 1142-1151.

[25] Ouyang Z and Liang J. Predicting protein folding rates from geometric contact and amino acid sequence. Protein Sci 2008; 17: 1256-1263.

[26] Dill KA, Ozkan SB, Weikl TR, Chodera JD and Voelz VA. The protein folding problem: when will it be solved? Curr Opin Struct Biol 2007; 17: 342-346.

[27] Khan SR and Denmeade SR. In vivo activity of a PSA-activated doxorubicin prodrug against PSA-producing human prostate cancer xenografts. Prostate 2000; 45: 80-83.

[28] Brady SF, Pawluczyk JM, Lumma PK, Feng DM, Wai JM, Jones R, DeFeo-Jones D, Wong BK, Miller-Stein C, Lin JH, Oliff A, Freidinger RM and Garsky VM. Design and synthesis of a pro-drug of vinblastine targeted at treatment of prostate cancer with enhanced efficacy and reduced

systemic toxicity. J Med Chem 2002; 45: 4706-4715.
[29] Graeser R, Chung DE, Esser N, Moor S, Schachtele C, Unger C and Kratz F. Synthesis and biological evaluation of an albumin-binding prodrug of doxorubicin that is cleaved by prostate-specific antigen (PSA) in a PSA-positive orthotopic prostate carcinoma model (LNCaP). Int J Cancer 2008; 122: 1145-1154.
[30] Gump JM and Dowdy SF. TAT transduction: the molecular mechanism and therapeutic prospects. Trends Mol Med 2007; 13: 443-448.
[31] Naresh A, Long W, Vidal GA, Wimley WC, Marrero L, Sartor CI, Tovey S, Cooke TG, Bartlett JM and Jones FE. The ERBB4/HER4 intracellular domain 4ICD is a BH3-only protein promoting apoptosis of breast cancer cells. Cancer Res 2006; 66: 6412-6420.
[32] Gan Y, Wientjes MG and Au JL. Expression of basic fibroblast growth factor correlates with resistance to paclitaxel in human patient tumors. Pharm Res 2006; 23: 1324-1331.
[33] Woollard DJ, Opeskin K, Coso S, Wu D, Baldwin ME and Williams ED. Differential expression of VEGF ligands and receptors in prostate cancer. Prostate 2012; 73: 563-572.
[34] Lin J and Kelly WK. Targeting angiogenesis as a promising modality for the treatment of prostate cancer. Urol Clin North Am 2012; 39: 547-560.
[35] Deezagi A, Ansari-Majd S and Vaseli-Hagh N. Induced apoptosis in human prostate cancer cells by blocking of vascular endothelial growth factor by siRNA. Clin Transl Oncol 2012; 14: 791-799.
[36] Montecinos VP, Godoy A, Hinklin J, Vethanayagam RR and Smith GJ. Primary xenografts of human prostate tissue as a model to study angiogenesis induced by reactive stroma. PLoS One 2012; 7: e29623.

Supplementary Table 1. PSA level of LNCaP and PC3 cell (ng/ml)*

Time	LNCaP		PC3	
	Cell culture	Cytoplasm	Cell culture	Cytoplasm
Day 1	8.8		0	
Day 2	25.81	82.83	0	0
Day 3	56.68	72.16	0.01	0.03
Day 4	96.61	190.6	0	0
Day 5	97.07	216.4	0	0

*Total PSA (T-PSA) were measured in 100 μl of the cell culture or cell lysis buffer (10^6 cells/1 ml lysis buffer).

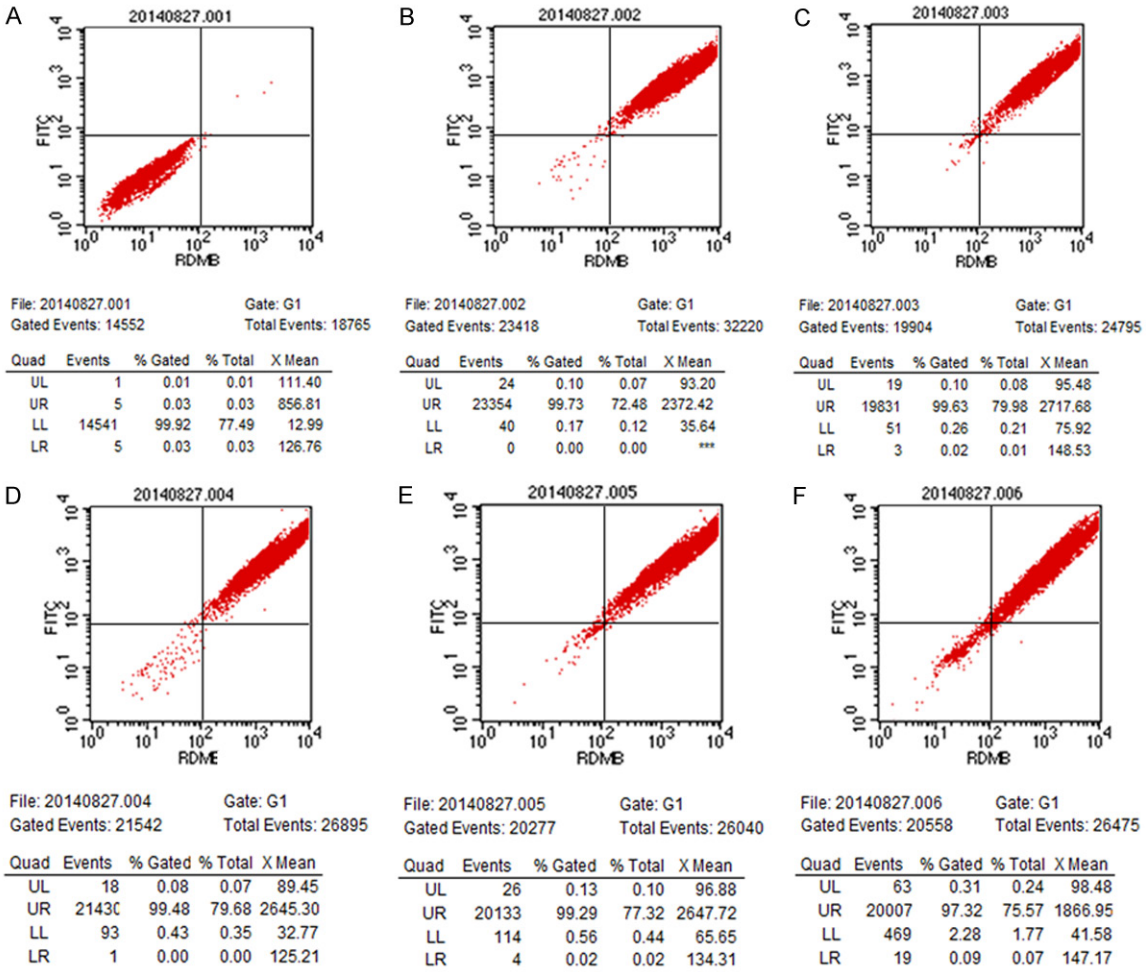

Supplementary Figure 1. Stability of APP8 in LNCaP cell. 50 μM FITC-labeled APP8 was added into cell culture of the LNCaP cell on 6-well plate. Then the cell was collected at 4 (B), 8 (C), 24 (D), 48 (E), and 72 (F) hrs with control (A) and flow cytometry was carried out to measure the fluorescence cells.

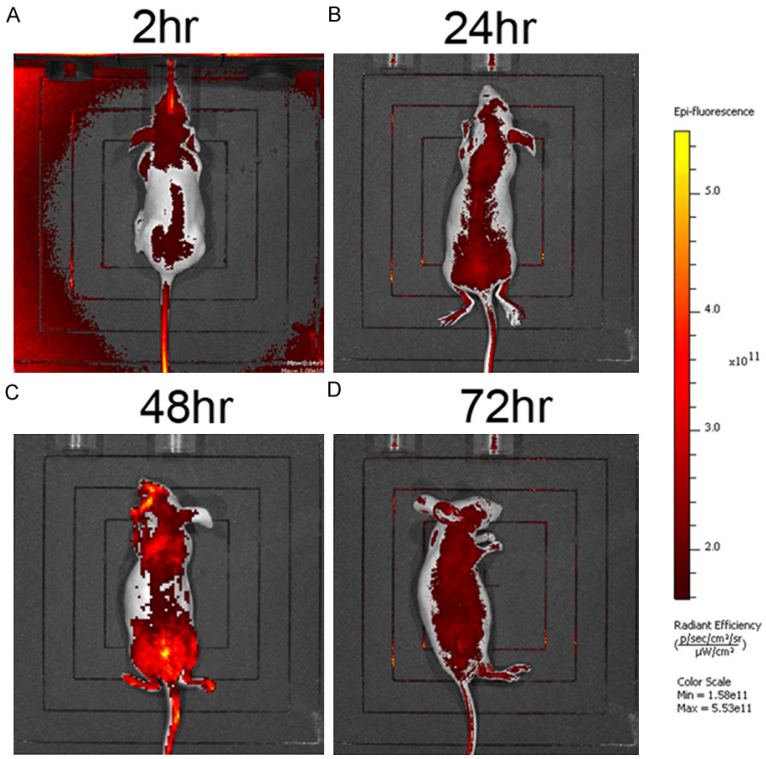

Supplementary Figure 2. Stability of APP8 in mice. 0.2 ml of 1 mM FITC-labeled APP8 was injected iv on LNCaP xenografts mice. Then animal vivo imaging was carried out on Caliper IVIS Lumina II (Caliper Life Sciences, Inc, USA) at 2 (A), 24 (B), 48 (C) and 72 (D) hrs later.